



1 **Influence of springtime atmospheric circulation types on the distribution of**  
2 **air pollutants in the Arctic**

3 Manu Anna Thomas<sup>1</sup>, Abhay Devasthale<sup>1</sup> and Tiina Nygård<sup>2</sup>

4 <sup>1</sup>Research and development, Swedish Meteorological and Hydrological Institute (SMHI),  
5 Folkborgsvägen 17, 60176 Norrköping, Sweden

6 <sup>2</sup>Polar Meteorology and Climatology Group, Finnish Meteorological Institute (FMI), Finland

7 Correspondence: [manu.thomas@smhi.se](mailto:manu.thomas@smhi.se)

8

9 **Abstract**

10 The transport and distribution of short-lived climate forcers in the Arctic is influenced by the  
11 prevailing atmospheric circulation patterns. Understanding the coupling between pollutant  
12 distribution and dominant atmospheric circulation types is therefore important, not least to  
13 understand the processes governing the local processing of pollutants in the Arctic, but also to test  
14 the fidelity of chemistry transport models to simulate the transport from the southerly latitudes.  
15 Here, we use a combination of satellite based and reanalysis datasets spanning over 12 years (2007-  
16 2018) and investigate the concentrations of NO<sub>2</sub>, O<sub>3</sub>, CO and aerosols and their co-variability during  
17 20 different atmospheric circulation types in the spring season (March, April and May) over the  
18 Arctic. We carried out a Self-Organizing Maps analysis of MSLP to derive these circulation types.

19 Although almost all pollutants investigated here show statistically significant sensitivity to the  
20 circulation types, NO<sub>2</sub> exhibits the strongest sensitivity among them. The circulation types with low-  
21 pressure systems located over the northeast Atlantic show a clear enhancement of NO<sub>2</sub> and AOD in  
22 the European Arctic. The O<sub>3</sub> concentrations are, however, decreased. The free tropospheric CO is  
23 increased over the Arctic during such events. The circulation types with atmospheric blocking over  
24 Greenland and northern Scandinavia show the opposite signal in which the NO<sub>2</sub> concentrations are  
25 decreased and AODs are smaller than the climatological values. The O<sub>3</sub> concentrations are, however,  
26 increased and the free tropospheric CO decreased during such events.

27 The study provides the most comprehensive assessment so far of the sensitivity of springtime  
28 pollutant distribution to the atmospheric circulation types in the Arctic and also provides an  
29 observational basis for the evaluation of chemistry transport models.

30



## 31 1. Introduction

32 The transport of anthropogenic pollutants from the southerly latitudes has many implications for the  
33 Arctic (Law and Stohl, 2007; Quinn et al., 2008; Shindell et al., 2008; Arnold et al., 2016; Willis et al.,  
34 2018; Abbatt et al., 2019; Schmale et al., 2021). At daily to weekly scales, the pollutants could exert  
35 an impact on the direct radiative forcing, thereby conditioning the atmospheric thermodynamics and  
36 influencing the surface energy budget. The transport of short-lived climate forcers (SLCFs), in  
37 particular, absorbing aerosols such as black carbon, is important in this context. The SLCFs can  
38 modulate the energy budget at shorter time scales, thereby possibly influencing the seasonal sea-ice  
39 evolution. Apart from their direct radiative effects, the SLCFs and other anthropogenic pollutants can  
40 also influence the cloud properties, exerting the so-called indirect effects. At climate time-scales,  
41 while mitigating the effects of increased carbon dioxide (CO<sub>2</sub>) and methane (CH<sub>4</sub>) could take many  
42 decades to even few hundred years, the regulation of SLCFs is considered as one of the effective  
43 strategies that could be implemented meanwhile to curb the overall impact of increasing greenhouse  
44 gases.

45 The Arctic Ocean is a very special region in this context, not only due to its geography and unique  
46 nature of environmental conditions, but also, due to the absence of any major sources of  
47 anthropogenic pollution in the central Arctic. The pollution sources are located either in the coastal  
48 zones or in the mid-latitude regions. This means that the net effect of SLCFs and the efficacy of their  
49 reduction measures depends heavily *on the atmospheric transport and the prevailing local*  
50 *atmospheric circulation patterns*, which could either dampen or favour the intended effects. This is  
51 also an area of research, where there exists a large knowledge gap currently. The uncertainties in  
52 model simulations of the impact of SLCFs on the Arctic are therefore high, limiting the design and  
53 assessment of the relevant reduction policies.

54 Pollutant transport to the Arctic occurs nearly all year round, and this transport is heavily influenced  
55 by large scale atmospheric circulation and various dynamical mechanisms, for example, cyclones,  
56 location of the storm track, high-latitude blockings, North Atlantic and Arctic Oscillations etc.  
57 (Messori et al. 2018; Papritz and Dunn-Sigouin, 2020), as well as the local environmental and  
58 meteorological conditions (for example, structure of the atmospheric boundary layer, temperature  
59 and humidity inversions, the state of the sea-ice, clouds etc.) during different times of the year. In  
60 spring, the meteorological conditions in the Arctic are also usually more diverse than in the winter or  
61 the summer months, and the photochemistry begins to play an important role as the solar  
62 illumination conditions improve. The polar dome (Bozem et al. 2019), isolating cold air masses in the  
63 lower troposphere in the high Arctic from the rest of the Arctic, starts to weaken in spring, allowing



64 for more frequent exchange of air masses between the high Arctic and the lower latitudes. In  
65 addition to other anthropogenic sources, the pollutants from biomass burning are also being carried  
66 to the Arctic in spring (Stohl et al., 2007; Warneke et al., 2009, 2010). A host of studies have rightfully  
67 pointed out the existence, implications and importance of Arctic haze in shaping the Arctic weather  
68 and climate in the springtime. Hence, the spring season is a good test bed to investigate the coupling  
69 of prevailing weather states and the pollutant distribution in the Arctic. Furthermore, purely from the  
70 observational perspective, the availability of satellite-based observations from the sensors that rely  
71 on the solar channels increases in spring, as the improved solar illumination conditions allow the  
72 retrievals of trace gases.

73 In light of the reasons mentioned above, it is understandable that a number of major campaigns have  
74 been carried out in spring, providing valuable data and characterizing pollutant variability in relation  
75 to the transport and local meteorological conditions. The aircraft measurements, ARCTAS (Arctic  
76 Research of the Composition of the Troposphere from Aircraft and Satellites) and ARCPAC (Aerosol,  
77 Radiation, and Cloud Processes affecting Arctic Climate), among others, that were carried out as part  
78 of the POLARCAT (Polar Study using Aircraft, Remote Sensing, Surface Measurements and Models, of  
79 Climate, Chemistry, Aerosols and Transport) campaign for the spring and summer of 2008, provided  
80 a wealth of knowledge on Arctic pollution, the transport pathways and climate impacts (Law et al.,  
81 2014). This campaign period coincided with a variety of meteorological conditions that affected the  
82 transport of different pollutants into the Arctic. For example, ARCTAS data constrained with AIRS CO  
83 observations revealed that Arctic pollutants were dominated by European anthropogenic sources  
84 from surface to the free troposphere in some cases and by Asian anthropogenic sources above 2 km  
85 (Fisher et al., 2010, Jacob et al., 2010). The Asian transport pathways are mainly via the warm  
86 conveyor belts (Stohl, 2006). Low altitude ARCPAC flights also revealed increased pollutant  
87 concentrations, such as BC, throughout the Arctic atmospheric column during early spring of 2008,  
88 indicating accumulation of pollutants during the winter months due to lower temperatures, lack of  
89 solar radiation and stable stratification (Spackman et al., 2010). Also, Warneke et al., (2009)  
90 identified a significant influx of pollutants into Alaska from the forest fires in Russia and the  
91 agricultural burning in Asia. Modelling studies that followed these measurements estimated a  
92 reduction (0.8% in spring) in snow albedo over the Arctic owing to BC deposition originating from  
93 Russian fires (Wang et al., 2011).

94 The large-scale descend and stratospheric intrusions also play a role in the observed enhancement of  
95 pollutants. For example, BrO concentrations at lower levels were also noted to be enhanced as a  
96 result of intrusions of lower stratospheric air into the troposphere (Jacob et al., 2010). The enhanced  
97 BrO is also closely linked to frontal lifting in a polar cyclone in spring (Blechschmidt et al., 2016).



98 Despite a negative ENSO year, Arctic weather was strongly influenced by the Eurasian/North  
99 American anthropogenic or boreal fires (Brock et al., 2011; McNaughton et al., 2011) resulting in  
100 increased concentrations of CO and aerosol loading (van der Werf et al. 2010; de Villiers et al. 2010;  
101 Schmale et al. 2011; Quennehen et al. 2011; Di Pierro et al. 2013). Based on the aircraft  
102 measurements, Wespes et al., (2012) inferred that up to respectively 45 % and 60 % of the total O<sub>3</sub>  
103 and HNO<sub>3</sub> observed below 400 hPa over the Arctic were of European origin which is transported via  
104 northward and westerly trans-Siberian pathways. The contribution of these pollutants from the Asian  
105 and North American sectors to the Arctic was much weaker. Most recently, Thomas et al (2019)  
106 investigated the dependency of aerosol vertical distribution on the degree of atmospheric stability in  
107 the Arctic during winter and spring using the satellite observations. They argued that the observed  
108 dependency can be explained by the dominance of pollution transport within the boundary layer  
109 during winter and in the free troposphere during spring.

110 It is evident from the previous studies that a detailed assessment of the co-variability of atmospheric  
111 circulation types and pollutants is needed in the Arctic; a) to fully grasp the coupling between local  
112 meteorology, pollutant distribution and long-range transport in the Arctic, and b) to improve the  
113 representation of such co-variability and coupling in the models. Such assessment will also help to  
114 evaluate and better constraint the existing chemistry transport models as well as fully coupled Earth  
115 System models. In the present study, we therefore pose and seek answers to the following scientific  
116 questions:

- 117 1) Which typical atmospheric circulation types (CTs) prevail in the Arctic during springtime and  
118 what are the typical meteorological conditions associated with them?
- 119 2) How do these circulation types influence the distribution of trace gases such as NO<sub>2</sub>, O<sub>3</sub> and  
120 CO?
- 121 3) Is there a distinguishable signal in the aerosol distribution during these circulation types?

122

## 123 2. Observational datasets and methodology

124 We analysed the satellite-based datasets of NO<sub>2</sub>, CO and aerosols for March, April and May months  
125 from 2007 to 2018. These are based on retrievals from the Ozone Monitoring Instrument (OMI)  
126 onboard the NASA's Aura satellite, the hyperspectral Atmospheric Infrared Sounder (AIRS)  
127 instrument onboard the Aqua satellite and the Cloud and Aerosol Lidar with Orthogonal Polarization  
128 instrument onboard the CALIPSO satellite. All three satellites belong to the NASA's Afternoon Train  
129 (A-Train) convoy of the satellites, thus providing simultaneous observations in space and time. The  
130 ozone dataset is obtained from the Copernicus Atmospheric Monitoring Service (CAMS) reanalysis,



131 since the satellite-based observations of the lower tropospheric ozone or either not reliable or  
132 available.

133 Specifically, we analysed the AIRS Standard Daily IR-Only Version 7 and OMI OMNO2d Version 3  
134 products. We use AIRS CO retrievals at 500 hPa and total column OMI NO<sub>2</sub> retrievals. Furthermore,  
135 we analysed O<sub>3</sub> at 925 hPa since the focus is on the near-surface O<sub>3</sub>. To investigate the tropospheric  
136 aerosol optical depths (AOD), the CALIPSO Level 2, standard aerosol profile product version 4.2  
137 available at 5 km horizontal resolution is used (CAL\_LID\_L2\_05kmAPro-Standard-V4-20). These  
138 datasets have been previously used to study the meteorological conditions and pollution variability in  
139 the high latitude regions, including the Arctic (Devasthale et al., 2011; Devasthale and Thomas, 2012;  
140 Thomas and Devasthale, 2014; Devasthale et al., 2016; Thomas and Devasthale, 2017; Thomas et al.,  
141 2019). We analyse the retrievals designated Tqj in the AIRS product as they are of best quality and  
142 are suitable for process and climate studies. In the case of CALIPSO APro product, we select data only  
143 when the Cloud-Aerosol-Discrimination Score is between and equal to (-50, -100) and when the  
144 Extinction Quality flag is 0, 1 or 2. For all satellite products, the data from the ascending passes  
145 (daytime conditions) are used.

146 The dominant CTs in the Arctic in spring were identified and clustered by applying the Self-Organizing  
147 Map (SOM) method, developed by Kohonen (2001). The SOM method uses unsupervised learning to  
148 determine generalized patterns in input data, and the method has previously been utilized to  
149 statistically cluster synoptic weather patterns (e.g., Hewitson and Crane 2002; Cassano et al. 2006;  
150 Gibson et al. 2017; Nygård et al. 2019). In this study, we allocated 20 characteristic atmospheric  
151 circulation types in spring (MAM, 2007–2018), using mean sea-level pressure (MSLP) data of ERA5  
152 reanalysis (Copernicus Climate Change Service, 2017) produced by the European Centre for Medium-  
153 Range Weather Forecasts at 6 h interval as the input data. In the initial phase of the SOM analysis,  
154 each of the 20 nodes in the SOM array had an associated reference vector with an equal dimension  
155 to the input MSLP data. Then, each time step of input MSLP data was compared with the reference  
156 vector of each node during the SOM training. The reference vectors, which were most similar to the  
157 input data vector, were adjusted towards the input data vector. This procedure was repeated until  
158 the reference vectors did not change anymore. As an output, a two-dimensional SOM array of  
159 gridded MSLP fields, having probability density of the input MSLP data, was obtained. This array was  
160 organized according to similarities in CTs, having the most similar circulation patterns located next to  
161 each other and the most dissimilar patterns in the corners of the array. Each time step of the input  
162 MSLP data was linked to the most similar circulation type or weather state (node) in the array. Based  
163 on these time steps, we were also able to form composites of trace gases in each CT separately.



164 After deriving the prevalent circulation types, we computed the climatological means of NO<sub>2</sub>, CO, O<sub>3</sub>  
165 and AOD during the March, April and May months separately. For each circulation type, the number  
166 of days that represent that type could be different in each month. In order to compute a  
167 climatological mean that takes in to account this difference, we weighed the climatological means of  
168 each month with weighing factors shown in Fig. 1, giving climatological means of NO<sub>2</sub>, CO, O<sub>3</sub> and  
169 AOD associated with each weather state. We then computed composites of NO<sub>2</sub>, CO, O<sub>3</sub> and AOD for  
170 each weather state. The anomalies shown later are the differences between these composites and  
171 the weighted climatological means for each weather state. Only those anomalies that are statistically  
172 significant using Student's t test at 90% confidence interval are shown.

173

### 174 **3. Overview of the CTs and associated meteorological conditions**

175 Fig. 2 shows the mean MSLP patterns during the 20 CTs that emerge from the SOM analysis. These  
176 types are mainly characterized by different locations and strengths of cyclones and anticyclones with  
177 respect to one another. For example, the first CT (CT1) is characterized by the most commonly  
178 observed low pressure regimes in the Northeast Atlantic and European Arctic and an intense  
179 Beaufort high on the Pacific side of the Arctic. In CT2 to CT4, the low pressure systems in the  
180 Greenland and Norwegian Seas gradually intensify, while the anticyclone moves over the Chukchi  
181 and East Siberian seas and weaken in their intensity. An intense high over the Beaufort Sea is  
182 observed in CT5 together with low pressure systems that move over the Barents and Kara Seas. In  
183 CT6, the anticyclone extends further north in to central Arctic. In the cases of CT9, CT13, CT14, CT17,  
184 almost half of the Arctic (Greenland, Canadian archipelago and Beaufort Sea and Alaska) is under the  
185 influence of a strong anticyclone, with the center of action moving east-west of the international  
186 date line. The strongest anticyclonic conditions are observed during CT13, while the strongest  
187 cyclonic conditions are observed in CT4 over the Greenland and Norwegian Seas. CT11 has on the  
188 other hand least spatial MSLP variability. The SOM analysis presented in Fig 2 reveals how varied and  
189 complex the atmospheric large scale circulation is over the Arctic in spring.

190 Atmospheric circulation drives the transport in the atmosphere. For example, it largely distributes  
191 moisture in the Arctic atmosphere by dictating its horizontal transport and modulating the local  
192 evaporation at the surface. Fig. 3 shows the specific humidity anomalies ( $dq$ ), based on AIRS data,  
193 associated with those 20 CTs. These anomalies are a good indicator (and the manifestation) of the  
194 transport patterns shaped by the cyclonic and anticyclonic conditions mentioned above.  
195 Furthermore, atmospheric humidity has an impact on the aerosol optical properties and morphology.  
196 An increase in  $dq$  is seen in the Greenland and Norwegian Seas in CT1-CT4 due to the cyclonic



197 conditions in the Northeast Atlantic transporting more heat and moisture. In CT9 to CT13 and CT17,  
198 in the absence of such transport in the Northeast Atlantic and due to the presence of anticyclones  
199 over Greenland and Canadian archipelago, drier and cooler air masses are transported over the  
200 Greenland, Norwegian and Barents Seas. This is particularly noticeable in CT9, CT13 and CT17  
201 wherein the strength and extent of the anticyclone is very strong. In CT12, an increase in  $dq$  can be  
202 seen over the Laptev Sea as a result of the strong low pressure systems centered eastward of  
203 Scandinavia over the Barents and Kara Seas along the Russian coast.

204 Our results indicate that the CTs derived based on MSLP can also be used to analyze the free and  
205 upper tropospheric pollutants. The AIRS derived geopotential height anomalies at 500 hPa are shown  
206 in Fig. 4. There is a coupling between the lower and upper level circulation during those circulation  
207 types and, especially, a good resemblance in the locations of the centers of action of low pressure  
208 systems and anticyclones derived based on MSLP and the 500 hPa geopotential heights.

209

#### 210 **4. Co-variability of CTs and air pollutants**

211 The response of  $\text{NO}_2$  to the CTs is shown in Fig. 5 in terms of weighted anomalies. It is to be noted  
212 that, while the SOM analysis is done over the region northward of 60N in order to emphasize the  
213 circulation patterns in the Arctic region, we present the anomalies of the pollutants northward of  
214 50N in order to provide the large-scale spatial context. It can be seen that the spatial distribution of  
215  $\text{NO}_2$  is highly sensitive to the CTs, not only over the polluted mainland and source regions, but also  
216 over the Arctic Ocean. Particularly over northern Europe, a distinct pattern emerges, wherein the  
217  $\text{NO}_2$  anomalies change sign gradually from CT1 to CT20 in response to the changing atmospheric  
218 circulation patterns. In CT1 to CT4, there is a clear transport signal in the  $\text{NO}_2$  anomalies. The location  
219 of low pressure systems in the Northeast Atlantic favors the transport of  $\text{NO}_2$  from the northern,  
220 central and eastern European regions into the Arctic. The increased specific humidity anomalies in  
221 the European Arctic further confirm such a transport (Fig. 3). The strongest signal is observed in CT4,  
222 when the center of action of polar vortex is located over Greenland (Figs. 2 and 4) and the intensity  
223 of the vortex is also very high, favouring the increased transport of  $\text{NO}_2$  in the Barents and Kara Seas,  
224 reaching even further north into the Arctic. Previous studies have indicated that, in the European  
225 sector of the Arctic, such transport occurs predominantly in the lower troposphere (Stohl, 2006;  
226 Thomas et al., 2019). A pronounced increase in humidity anomalies is also seen over these regions in  
227 CT4. Among all circulation types, the highest  $\text{NO}_2$  anomalies are observed over Scandinavia in CT1-  
228 CT4, suggesting a noticeable influence of these circulation types in the pollution variability in these  
229 countries. The transport from the central and eastern European countries is especially predominant



230 in CT4. It is to be noted that the circulation types, CT1 to CT4 roughly resemble the typical loading  
231 patterns of North Atlantic Oscillation and/or Arctic Oscillations over the central and Eurasian Arctic,  
232 which is shown to have a noticeable impact on the pollutant variability over these regions (e.g.  
233 Eckhardt et al., 2003; Christoudias et al., 2012).

234 An entirely opposite NO<sub>2</sub> response is seen in CT14 to CT19. In cases, CT14 and CT17 with anticyclonic  
235 conditions prevailing over Greenland and northern north Atlantic at varying intensity, the transport  
236 of cleaner air masses from the central Arctic lead to negative NO<sub>2</sub> anomalies over the central and  
237 northern parts of Europe. In CT14 to CT19, the anticyclone moves eastwards over Greenland and  
238 Norwegian Seas and over northern Scandinavia, blocking the transport from the southerly latitudes  
239 and therefore leading to negative NO<sub>2</sub> anomalies during these circulation types as well. Furthermore,  
240 in CT15, CT18 and CT19, this circulation pattern in Canadian archipelago and European sector of the  
241 Arctic, together with cyclonic conditions in central and Eastern Siberian regions facilitate the north  
242 east Asian transport of NO<sub>2</sub> into Alaska and northern Canada. Among all CTs, CT11 has the lowest  
243 anomalies in the NO<sub>2</sub> concentrations, in conjunction with very mild changes in the MSLP during this  
244 CT. The northeast Asian regions and northern Pacific Ocean show no sensitivity to the circulation  
245 types, most likely due to the persistent nature of westerly winds over this region in combination with  
246 the persistent continental pollution outflow over the northern Pacific.

247 The O<sub>3</sub> anomalies at 925 hPa also show sensitivity to the circulation types. They appear to be  
248 opposite in nature to that of the NO<sub>2</sub> anomalies. For example, a reduction in the O<sub>3</sub> concentrations  
249 over northeast Atlantic and Scandinavia seen in CT1-CT4 is consistent with the strong NO<sub>2</sub> increases  
250 observed during the same circulation types. A statistically significant increase in central Arctic is seen  
251 in CT1, CT5, CT9 and CT13. However, the corresponding NO<sub>2</sub> anomalies over central Arctic in these  
252 circulation types are not statistically significant. An inverse correspondence between O<sub>3</sub> and NO<sub>2</sub>  
253 away from the source regions is not expected due to the different life times, aging and transport  
254 processes. A decrease in O<sub>3</sub> concentrations over central Arctic corresponds to the presence of  
255 cyclonic conditions over Eurasia and Siberia (CT15, CT16, CT18-CT20).

256 The springtime photochemistry in the Arctic is very complex, as duly noted in the rich literature that  
257 documents the research and observations on this subject matter (Lu et al., 2019 and the references  
258 therein). The interactions between NO<sub>2</sub> and O<sub>3</sub> are also highly non-linear in reality and hence a one-  
259 one correlation can not be established. In the troposphere, NO is converted to NO<sub>2</sub> in the presence of  
260 O<sub>3</sub> which is a potential sink for O<sub>3</sub>. However, during sun-lit conditions, NO<sub>2</sub> is converted back to NO  
261 via photolysis which results in O<sub>3</sub> production. Apart from these chemical reactions, local  
262 meteorological conditions such as temperature, relative humidity, rainfall play an important role in





263 the production and dispersion of these pollutants. Stratospheric intrusions are another source of O<sub>3</sub>  
264 variability in the troposphere that may play a role under different circulation types (Yates et al.,  
265 2013; Langford et al., 2015; Lin et al., 2015). The persistent anticyclonic conditions could, not only  
266 lead to the accumulation of the tropospheric O<sub>3</sub>, but also favour the large-scale descend or intrusions  
267 into the lower troposphere, leading to positive O<sub>3</sub> anomalies.

268 Fig. 7 shows the tropospheric AOD anomalies based on the CALIOP-CALIPSO aerosol profile product.  
269 It is to be noted that, being an active profiler, the spatial coverage of CALIOP-CALIPSO is very poor  
270 and the anomalies look patchy, particularly over the inland regions because of a limited number of  
271 samples for each weather state. The passive imagers either do not have AOD data available in spring  
272 (due to poor illumination conditions) or the quality of the retrievals can be very poor due to the  
273 challenging surface conditions and the underlying uncertainties in cloud masking. CALIOP provides  
274 the most accurate sampling of aerosols over the Arctic Ocean in spring in comparison to passive  
275 imagers, but with this trade-off of having poor spatial sampling and therefore the AOD data have to  
276 be interpreted cautiously. We, nonetheless, decided to include CALIPSO in the analysis since it can  
277 provide an important context while studying the trace gas variability. For example, we can see that  
278 there are at least two signals that are robust and consistent with other observations. An increase in  
279 AOD in CT1 to CT4 is observed in Greenland and Norwegian Seas and northern Scandinavia, which is  
280 consistent with the increases in NO<sub>2</sub>, further confirming the role of these circulation types in  
281 transporting the pollutants in to the Arctic. It is to be noted that the humidity also increases from CT1  
282 to CT4 and will have an impact on the AODs due to increased water uptake during transport. These  
283 circulation types are similar to those that could change the stability regimes as a result of heat and  
284 moisture transport over the colder sea-ice surfaces in the inner Arctic and trapping the aerosols and  
285 pollutants below the inversions in the Eurasian sector of the Arctic, as previously reported in Thomas  
286 et al., 2019. The opposite tendencies in CT13, CT14, CT15, CT17 and CT18, wherein the negative AOD  
287 anomalies are observed over the Norwegian Sea and northern Scandinavia, are also consistent with  
288 the NO<sub>2</sub> decreases observed in these circulation types. The anticyclones prevailing over Greenland  
289 and north of Scandinavia block the transport of trace gases and aerosols in to the Arctic during these  
290 circulation patterns. The increased AODs along the western coast of Scandinavia in CT9 could be due  
291 to the location of anticyclone in the Arctic and the low pressure systems in central Europe that  
292 transport pollutants from the eastern Europe and western parts of Russia, including the biomass  
293 burning regions, over these coastal regions. In the case of other circulation types, the AOD anomalies  
294 are too patchy to draw meaningful conclusions in the sense that there are no consistent features  
295 either with the meteorological conditions or other pollutants.



296 Unlike tropospheric O<sub>3</sub> and NO<sub>2</sub>, CO has the atmospheric lifetime ranging from few weeks to few  
297 months and therefore is often regarded as a suitable tracer to study the long-range pollution  
298 transport. Due to its longevity, the spatial distribution of CO in the free troposphere is also quite  
299 homogeneous compared to other trace gases and the local pollution variability is often diffused in  
300 the large-scale signal. However, CO is an excellent tracer to study the coupling between the pollution  
301 variability in the free troposphere and the lower tropospheric circulation patterns, given the  
302 influence of these CTs on the entire troposphere, and also to study the large-scale, first order impact  
303 of the CTs on the free tropospheric pollutants. Such a large-scale signal is indeed visible in the CO  
304 anomalies shown in Fig. 8. Two main regimes can be seen; one dominated by the Arctic-wide  
305 increases in the CO concentrations (eg. CT1 to CT4) when the low pressure systems are active in the  
306 North Atlantic and the other when the decreases in the CO concentrations (eg. CT14, CT15, CT18 and  
307 CT19) can be seen over much of the Arctic likely due to the atmospheric blocking over those regions.  
308 The CO anomalies over Scandinavia, northeast Atlantic, Greenland, Norwegian and Barents Seas  
309 show strongest sensitivity to the circulation types.

310

## 311 5. Conclusions

312 The transport and the distribution of the pollutants in the Arctic, especially that of the short-lived  
313 climate forcers, depends heavily on the prevailing atmospheric circulation patterns. Understanding  
314 pollutant variability in relation to the dominant circulation types is therefore important. Here, we  
315 investigate the concentrations of NO<sub>2</sub>, O<sub>3</sub>, CO and aerosols and their co-variability during the 20  
316 different circulation types in the spring season (March, April and May) over the Arctic. The circulation  
317 types discussed in this study are derived by the Self-Organizing Maps analysis of MSLP. A  
318 combination of satellite based and reanalysis datasets spanning over 12 years (2007-2018) is used.  
319 The following conclusions are drawn from the analysis.

320 a) The 20 characteristic circulation patterns during spring, allocated by the SOM analysis based on  
321 the MSLP fields, represent different locations and intensities of cyclonic and anticyclonic events in  
322 relation to each other. The MSLP circulation patterns are connected to 500 hPa geopotential height  
323 anomalies and also shape the atmospheric humidity distribution. The circulation patterns largely  
324 dictate the transport in the atmosphere, especially from the main source areas in the southerly  
325 latitudes.

326 b) It is observed that all pollutants investigated here show sensitivity to the circulation types and  
327 some common patterns emerge in their response. NO<sub>2</sub> shows the strongest sensitivity among the  
328 trace gases and aerosols analyzed here.



329 c) The circulation types (CT1 to CT4) with low-pressure systems located in the northeast Atlantic  
330 show a clear statistically significant enhancement of NO<sub>2</sub> and AOD in the European Arctic. The O<sub>3</sub>  
331 concentrations are however decreased in such events.

332 d) The circulation types (CT14, CT15, CT18 and CT19) with atmospheric blocking over Greenland and  
333 northern Scandinavia show the opposite signal, in that the NO<sub>2</sub> concentrations are decreased and  
334 AODs are smaller than the climatological values. The O<sub>3</sub> concentrations are however increased during  
335 these events in the European Arctic.

336 e) The first order signal of the influence of circulation types on the free tropospheric CO is seen, with  
337 two main regimes emerging. The first regime shows the Arctic-wide positive anomalies in the CO  
338 concentrations when the low pressure systems are active in the North Atlantic and the other when  
339 the negative CO anomalies are observed due to the atmospheric blocking over those regions.

340

341 The present study provides the most comprehensive investigations so far of the sensitivity of  
342 springtime pollutant distribution to the atmospheric circulation types in the Arctic, also providing an  
343 observational basis for the evaluation of chemistry transport models.

344

#### 345 **Acknowledgements**

346 The study was funded by the Swedish National Space Agency (grant number 94/16). The authors  
347 would like to thank the OMI, AIRS and CALIPSO Science Teams for the data products as well as CAMS  
348 and ECMWF for the corresponding reanalysis data products.

#### 349 **Code/Data availability**

350 All datasets used in the present study are publicly available below:

351 [https://disc.gsfc.nasa.gov/datasets/OMNO2G\\_003/summary](https://disc.gsfc.nasa.gov/datasets/OMNO2G_003/summary)

352 <https://airs.jpl.nasa.gov/data/get-data/standard-data/>

353 <https://atmosphere.copernicus.eu/data>

#### 354 **Competing interests**

355 The authors declare no competing interests.

356



357 **Author contributions**

358 MT and AD designed the study. MT carried out the analysis and wrote the first draft of the  
359 manuscript. TN performed and provided the SOM analysis. All authors contributed to the writing and  
360 interpretation of the results.

361 **References**

- 362 Abbatt, J. P. D. et al., New insights into aerosol and climate in the Arctic, *Atmos. Chem. Phys.*, **19**,  
363 2527–2560, <https://doi.org/10.5194/acp-19-2527-2019>, 2019.
- 364 Arnold, S. R., K.S. Law, C.A. Brock, J.L. Thomas, S.M. Starkweather, K. von Salzen, A. Stohl, S. Sharma,  
365 M.T. Lund, M.G. Flanner, T. Petäjä, H. Tanimoto, J. Gamble, J.E. Dibb, M. Melamed, N. Johnson, M.  
366 Fidel, V.-P. Tynkkynen, A. Baklanov, S. Eckhardt, S.A. Monks, J. Browse, H. Bozem; Arctic air pollution:  
367 Challenges and opportunities for the next decade. *Elementa: Science of the Anthropocene* 1 January  
368 2016; 4 000104. doi: <https://doi.org/10.12952/journal.elementa.000104>
- 369 Blechschmidt, A.-M., Richter, A., Burrows, J. P., Kaleschke, L., Strong, K., Theys, N., Weber, M., Zhao,  
370 X., and Zien, A.: An exemplary case of a bromine explosion event linked to cyclone development in  
371 the Arctic, *Atmos. Chem. Phys.*, **16**, 1773–1788, <https://doi.org/10.5194/acp-16-1773-2016>, 2016.
- 372 Bozem, H., Hoor, P., Kunkel, D., Köllner, F., Schneider, J., Herber, A., Schulz, H., Leaitch, W. R.,  
373 Aliabadi, A. A., Willis, M. D., Burkart, J., and Abbatt, J. P. D., (2019): Characterization of transport  
374 regimes and the polar dome during Arctic spring and summer using in situ aircraft measurements,  
375 *Atmos. Chem. Phys.*, **19**, 15049–15071, <https://doi.org/10.5194/acp-19-15049-2019>.
- 376 Brock, C. A., Cozic, J., Bahreini, R., Froyd, K. D., Middlebrook, A. M., McComiskey, A., Brioude, J.,  
377 Cooper, O. R., Stohl, A., Aikin, K. C., de Gouw, J. A., Fahey, D. W., Ferrare, R. A., Gao, R.-S., Gore, W.,  
378 Holloway, J. S., Hübler, G., Jefferson, A., Lack, D. A., Lance, S., Moore, R. H., Murphy, D. M., Nenes, A.,  
379 Novelli, P. C., Nowak, J. B., Ogren, J. A., Peischl, J., Pierce, R. B., Pilewskie, P., Quinn, P. K., Ryerson, T.  
380 B., Schmidt, K. S., Schwarz, J. P., Sodemann, H., Spackman, J. R., Stark, H., Thomson, D. S., Thornberry,  
381 T., Veres, P., Watts, L. A., Warneke, C., and Wollny, A. G., (2011): Characteristics, sources, and  
382 transport of aerosols measured in spring 2008 during the aerosol, radiation, and cloud processes  
383 affecting Arctic Climate (ARCPAC) Project, *Atmos. Chem. Phys.*, **11**, 2423–2453,  
384 <https://doi.org/10.5194/acp-11-2423-2011>.
- 385 Cassano, J. J., Uotila, P. and Lynch, A., (2006): Changes in synoptic weather patterns in the polar regions  
386 in the twentieth and twenty-first centuries, part 1: Arctic, *Int. J. Climatol.*, **26**, 1027-1049,  
387 <https://doi.org/10.1002/joc.1306>.



- 388 Christoudias, T., Pozzer, A., and Lelieveld, J., (2012): Influence of the North Atlantic Oscillation on air  
389 pollution transport, *Atmos. Chem. Phys.*, 12, 869–877, <https://doi.org/10.5194/acp-12-869-2012>
- 390 Copernicus Climate Change Service (C3S), 2017: ERA5: Fifth generation of ECMWF atmospheric  
391 reanalyses of the global climate. Copernicus Climate Change Service Climate Data Store (CDS),  
392 <https://cds.climate.copernicus.eu/cdsapp#!/home>
- 393 de Villiers, R. A., Ancellet, G., Pelon, J., Quennehen, B., Schwarzenboeck, A., Gayet, J. F., and Law, K. S.,  
394 (2010): Airborne measurements of aerosol optical properties related to early spring transport of mid-  
395 latitude sources into the Arctic, *Atmos. Chem. Phys.*, 10, 5011–5030, [https://doi.org/10.5194/acp-10-](https://doi.org/10.5194/acp-10-5011-2010)  
396 5011-2010.
- 397 di Pierro, M., Jaeglé, L., Eloranta, E. W., and Sharma, S., (2013): Spatial and seasonal distribution of  
398 Arctic aerosols observed by the CALIOP satellite instrument (2006–2012), *Atmos. Chem. Phys.*, 13,  
399 7075–7095, <https://doi.org/10.5194/acp-13-7075-2013>.
- 400 Devasthale, A. and Thomas, M. A., (2012): An investigation of statistical link between inversion  
401 strength and carbon monoxide over Scandinavia in winter using AIRS data, *Atmos. Environ.*, 56, 109–  
402 114, <https://doi.org/10.1016/j.atmosenv.2012.03.042>
- 403 Devasthale, A., Tjernstrom, M., Karlsson, K.-G., Thomas, M. A., Jones, C., Sedlar, J., & Omar, A. H.  
404 (2011). The vertical distribution of thin features over the Arctic analysed from CALIPSO observations  
405 part II: Aerosols. *Tellus Series B: Chemical and Physical Meteorology*, 63(1), 86–95.  
406 <https://doi.org/10.1111/j.1600-0889.2010.00517.x>
- 407 Devasthale, A., Sedlar, J., Kahn, B., Tjernström, M., Fetzner, E., Tian, B., Teixeira, J., & Pagano, T.  
408 (2016). A decade of spaceborne observations of the Arctic atmosphere: Novel insights from NASA's  
409 AIRS instrument. *Bulletin of the American Meteorological Society*, 97(11), 2163–2176.  
410 <https://doi.org/10.1175/BAMS-D-14-00202.1>
- 411 Eckhardt, S., Stohl, A., Beirle, S., Spichtinger, N., James, P., Forster, C., Junker, C., Wagner, T., Platt, U.,  
412 and Jennings, S. G., (2003): The North Atlantic Oscillation controls air pollution transport to the  
413 Arctic, *Atmos. Chem. Phys.*, 3, 1769–1778, <https://doi.org/10.5194/acp-3-1769-2003>
- 414 Fisher, J. A., Jacob, D. J., Purdy, M. T., Kopacz, M., Le Sager, P., Carouge, C., Holmes, C. D., Yantosca,  
415 R. M., Batchelor, R. L., Strong, K., Diskin, G. S., Fuelberg, H. E., Holloway, J. S., Hyer, E. J., McMillan, W.  
416 W., Warner, J., Streets, D. G., Zhang, Q., Wang, Y., and Wu, S., (2010): Source attribution and  
417 interannual variability of Arctic pollution in spring constrained by aircraft (ARCTAS, ARCPAC) and



- 418 satellite (AIRS) observations of carbon monoxide, *Atmos. Chem. Phys.*, **10**, 977–996,  
419 <https://doi.org/10.5194/acp-10-977-2010>
- 420 Gibson, P. B., Perkins-Kirkpatrick, S. E., Uotila, P., Pepler, A. S., and Alexander, L. V. (2017), On the use  
421 of self-organizing maps for studying climate extremes, *J. Geophys. Res. Atmos.*, **122**, 3891– 3903,  
422 <https://doi.org/10.1002/2016JD026256>
- 423 Hewitson, B. C., and Crane, R. G., (2002): Self-organizing maps: applications to synoptic climatology,  
424 *Clim. Res.*, **22**, 13-26.
- 425 Jacob, D. J., Crawford, J. H., Maring, H., Clarke, A. D., Dibb, J. E., Emmons, L. K., Ferrare, R. A.,  
426 Hostetler, C. A., Russell, P. B., Singh, H. B., Thompson, A. M., Shaw, G. E., McCauley, E., Pederson, J.  
427 R., and Fisher, J. A., (2010): The Arctic Research of the Composition of the Troposphere from Aircraft  
428 and Satellites (ARCTAS) mission: design, execution, and first results, *Atmos. Chem. Phys.*, **10**, 5191–  
429 5212, <https://doi.org/10.5194/acp-10-5191-2010>
- 430 Kohonen, T., (2001): *Self-Organizing Maps*. Springer-Verlag, 501 pp.
- 431 Langford, A. O., Senff, C. J., Alvarez, R. J., Brioude, J., Cooper, O. R., Holloway, J. S., Lin, M. Y.,  
432 Marchbanks, R. D., Pierce, R. B., Sandberg, S. P., Weickmann, A. M. and Williams, E. J. (2015). An  
433 overview of the 2013 Las Vegas Ozone Study (LVOS): Impact of stratospheric intrusions and long-  
434 range transport on surface air quality. *Atmospheric Environment*, **109**, 305–322.  
435 <https://doi.org/10.1016/j.atmosenv.2014.08.0>
- 436 Law, K. S., and A. Stohl (2007), Arctic air pollution: Origins and impacts, *Science*, **315**, 1537–1540.
- 437 Law, K. S., Stohl, A., Quinn, P. K., Brock, C. A., Burkhardt, J. F., Paris, J., Ancellet, G., Singh, H. B., Roiger,  
438 A., Schlager, H., Dibb, J., Jacob, D. J., Arnold, S. R., Pelon, J., & Thomas, J. L. (2014). Arctic Air  
439 Pollution: New Insights from POLARCAT-IPY, *Bulletin of the American Meteorological Society*, **95**(12),  
440 1873-1895.
- 441 Lin, M., Fiore, A. M., Horowitz, L. W., Langford, A. O., Oltmans, S. J., Tarasick, D. and Rieder, H. E.  
442 (2015): Climate variability modulates western US ozone air quality in spring via deep stratospheric  
443 intrusions. *Nat. Commun.*, <https://doi.org/10.1038/ncomms8105>.
- 444 Lu, X., Zhang, L. and Shen, L. (2019): Meteorology and Climate Influences on Tropospheric Ozone: a  
445 Review of Natural Sources, Chemistry, and Transport Patterns. *Current Pollution Reports*.  
446 <https://doi.org/10.1007/s40726-019-00118-3>.
- 447 McNaughton, C. S., Clarke, A. D., Freitag, S., Kapustin, V. N., Kondo, Y., Moteki, N., Sahu, L.,  
448 Takegawa, N., Schwarz, J. P., Spackman, J. R., Watts, L., Diskin, G., Podolske, J., Holloway, J. S.,



- 449 Wisthaler, A., Mikoviny, T., de Gouw, J., Warneke, C., Jimenez, J., Cubison, M., Howell, S. G.,  
450 Middlebrook, A., Bahreini, R., Anderson, B. E., Winstead, E., Thornhill, K. L., Lack, D., Cozic, J., and  
451 Brock, C. A., (2011): Absorbing aerosol in the troposphere of the Western Arctic during the 2008  
452 ARCTAS/ARCPAC airborne field campaigns, *Atmos. Chem. Phys.*, 11, 7561–7582,  
453 <https://doi.org/10.5194/acp-11-7561-2011>.
- 454 Messori, G., Woods, C., & Caballero, R. (2018). On the drivers of wintertime temperature extremes in  
455 the high Arctic. *Journal of Climate*, 31, 1597– 1618. <https://doi.org/10.1175/JCLI-D-17-0386.1>
- 456 Nygård, T., Graversen, R. G., Uotila, P., Naakka, T., & Vihma, T. (2019). Strong Dependence of  
457 Wintertime Arctic Moisture and Cloud Distributions on Atmospheric Large-Scale Circulation, *Journal*  
458 *of Climate*, 32(24), 8771-8790.
- 459 Papritz, L., Dunn-Sigouin, E. (2020). What configuration of the atmospheric circulation drives extreme  
460 net and total moisture transport into the Arctic. *Geophysical Research Letters*, 47, e2020GL089769.  
461 <https://doi.org/10.1029/2020GL089769>  
462
- 463 Quennehen, B., Schwarzenboeck, A., Schmale, J., Schneider, J., Sodemann, H., Stohl, A., Ancellet, G.,  
464 Crumeyrolle, S., and Law, K. S., (2011): Physical and chemical properties of pollution aerosol particles  
465 transported from North America to Greenland as measured during the POLARCAT summer campaign,  
466 *Atmos. Chem. Phys.*, 11, 10947–10963, <https://doi.org/10.5194/acp-11-10947-2011>.
- 467 Quinn, P. K., et al. (2008), Short-lived pollutants in the Arctic: their climate impact and possible  
468 mitigation strategies, *Atmos. Chem. Phys.*, 8, 1723–1735.
- 469 Schmale, J., Zieger, P. & Ekman, A.M.L. Aerosols in current and future Arctic climate. *Nat. Clim.*  
470 *Chang.* 11, 95–105 (2021). <https://doi.org/10.1038/s41558-020-00969-5>
- 471 Shindell, D. T., et al. (2008), A multi-model assessment of pollution transport to the Arctic, *Atmos.*  
472 *Chem. Phys.*, 8, 5353–5372.
- 473 Schmale, J., Schneider, J., Ancellet, G., Quennehen, B., Stohl, A., Sodemann, H., Burkhardt, J. F.,  
474 Hamburger, T., Arnold, S. R., Schwarzenboeck, A., Borrmann, S., and Law, K. S., (2011): Source  
475 identification and airborne chemical characterisation of aerosol pollution from long-range transport  
476 over Greenland during POLARCAT summer campaign 2008, *Atmos. Chem. Phys.*, 11, 10097–10123,  
477 <https://doi.org/10.5194/acp-11-10097-2011>.



- 478 Spackman, J. R., R. S. Gao, W. D. Neff, J. P. Schwarz, L. A. Watts, D. W. Fahey, J. S. Holloway, T. B.  
479 Ryerson, J. Peischl, and C. A. Brock (2010), Aircraft observations of enhancement and depletion of  
480 black carbon mass in the springtime Arctic, *Atmos. Chem. Phys.*, 10, 9667–9680.
- 481 Stohl, A. (2006), Characteristics of atmospheric transport into the Arctic troposphere, *J. Geophys.*  
482 *Res.*, 111, D11306, <https://doi.org/10.1029/2005JD006888>
- 483 Stohl, A., et al. (2007), Arctic smoke record high air pollution levels in the European Arctic due to  
484 agricultural fires in Eastern Europe in spring 2006, *Atmos. Chem. Phys.*, 7, 511–534.
- 485 Thomas, M. A. and Devasthale, A.: Sensitivity of free tropospheric carbon monoxide to atmospheric  
486 weather states and their persistency: an observational assessment over the Nordic countries, *Atmos.*  
487 *Chem. Phys.*, 14, 11545–11555, <https://doi.org/10.5194/acp-14-11545-2014>, 2014.
- 488 Thomas, M. A. and Devasthale, A.: Typical meteorological conditions associated with extreme  
489 nitrogen dioxide (NO<sub>2</sub>) pollution events over Scandinavia, *Atmos. Chem. Phys.*, 17, 12071–12080,  
490 <https://doi.org/10.5194/acp-17-12071-2017>, 2017.
- 491 Thomas, M. A., Devasthale, A., Tjernström, M., & Ekman, A. M. L. (2019). The relation between  
492 aerosol vertical distribution and temperature inversions in the Arctic in winter and spring.  
493 *Geophysical Research Letters*, 46, 2836– 2845. <https://doi.org/10.1029/2018GL081624>.
- 494 van der Werf, G. R., Randerson, J. T., Giglio, L., Collatz, G. J., Mu, M., Kasibhatla, P. S., Morton, D. C.,  
495 DeFries, R. S., Jin, Y., and van Leeuwen, T. T., (2010): Global fire emissions and the contribution of  
496 deforestation, savanna, forest, agricultural, and peat fires (1997–2009), *Atmos. Chem. Phys.*, 10,  
497 11707–11735, <https://doi.org/10.5194/acp-10-11707-2010>.
- 498 Wang, Q., Jacob, D. J., Fisher, J. A., Mao, J., Leibensperger, E. M., Carouge, C. C., Le Sager, P., Kondo,  
499 Y., Jimenez, J. L., Cubison, M. J., and Doherty, S. J., (2011): Sources of carbonaceous aerosols and  
500 deposited black carbon in the Arctic in winter-spring: implications for radiative forcing, *Atmos. Chem.*  
501 *Phys.*, 11, 12453–12473, <https://doi.org/10.5194/acp-11-12453-2011>.
- 502 Warneke, C., et al. (2009), Biomass burning in Siberia and Kazakhstan as an important source for haze  
503 over the Alaskan Arctic in April 2008, *Geophys. Res. Lett.*, 36, L02813,  
504 <https://doi.org/10.1029/2008GL036194>
- 505 Warneke, C., et al. (2010), An important contribution to springtime Arctic aerosol from biomass  
506 burning in Russia, *Geophys. Res. Lett.*, 37, L01801, doi:10.1029/2009GL041816.
- 507 Wespes, C., Emmons, L., Edwards, D. P., Hannigan, J., Hurtmans, D., Saunio, M., Coheur, P.-F.,  
508 Clerbaux, C., Coffey, M. T., Batchelor, R. L., Lindenmaier, R., Strong, K., Weinheimer, A. J., Nowak, J.





509 B., Ryerson, T. B., Crounse, J. D., and Wennberg, P. O., (2012): Analysis of ozone and nitric acid in  
510 spring and summer Arctic pollution using aircraft, ground-based, satellite observations and MOZART-  
511 4 model: source attribution and partitioning, Atmos. Chem. Phys., 12, 237–259,  
512 <https://doi.org/10.5194/acp-12-237-2012>

513 Willis, M. D., Leaitch, W. R., & Abbatt, J. P. (2018). Processes controlling the composition and  
514 abundance of Arctic aerosol. Reviews of Geophysics, 56, 621–671.  
515 <https://doi.org/10.1029/2018RG000602>

516 Yates, E. L., Iraci, L. T., Roby, M. C., Pierce, R. B., Johnson, M. S., Reddy, P. J., Tadić, J. M.,  
517 Loewenstein, M., and Gore, W. (2013). Airborne observations and modeling of springtime  
518 stratosphere-to-troposphere transport over California. Atmospheric Chemistry and Physics, 13(24),  
519 12,481–12,494. <https://doi.org/10.5194/acp-13-12481-2013>

520

521

522

523

524

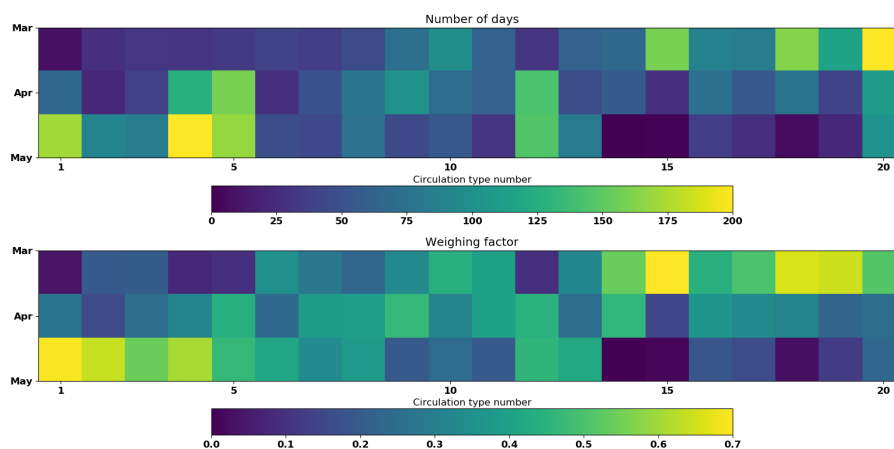
525

526

527

528

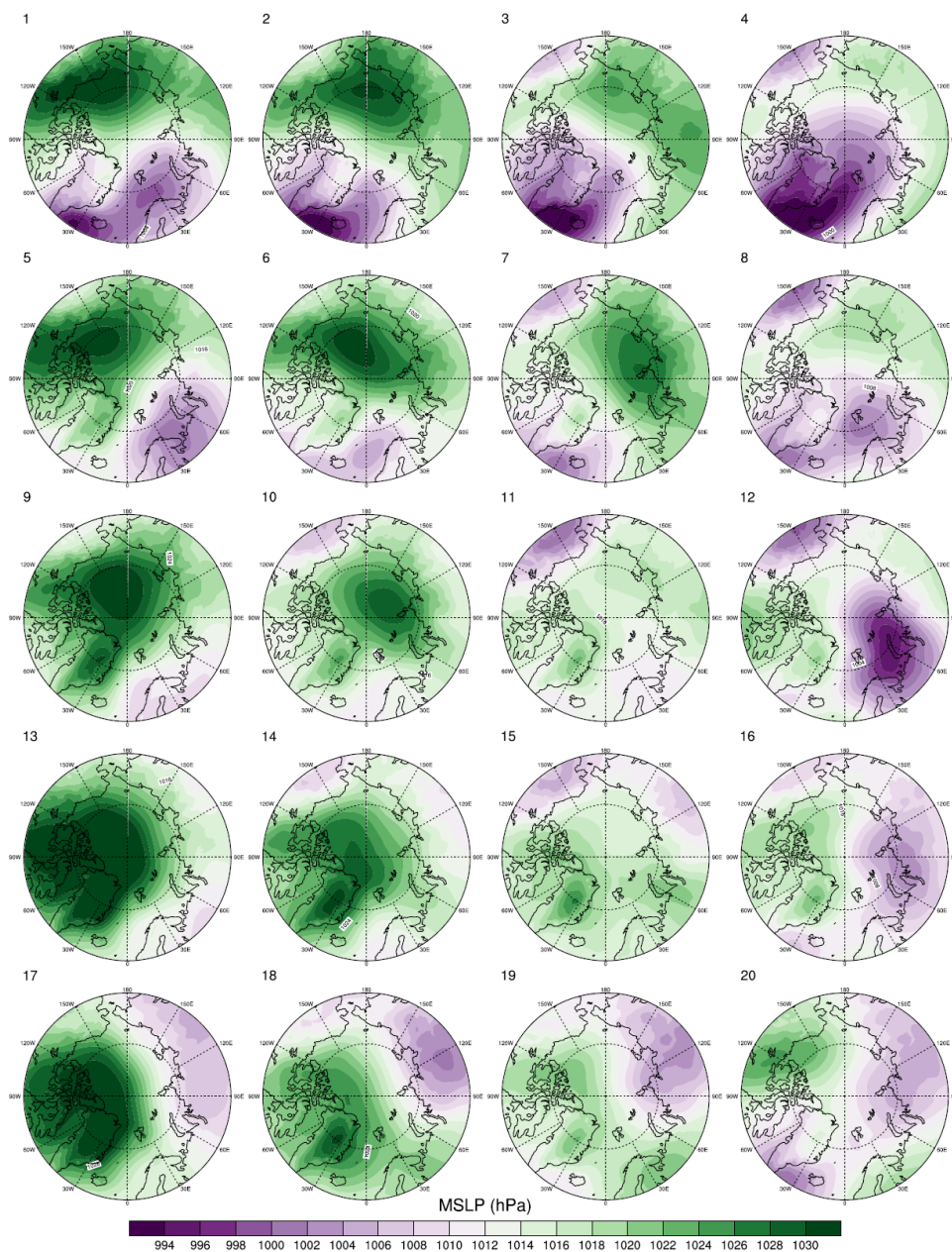
529



530

531 Fig. 1: a) The number of days analysed for each circulation type and month b) the corresponding  
532 weighing factor used to compute the climatologies of trace gases and aerosols.

533



534

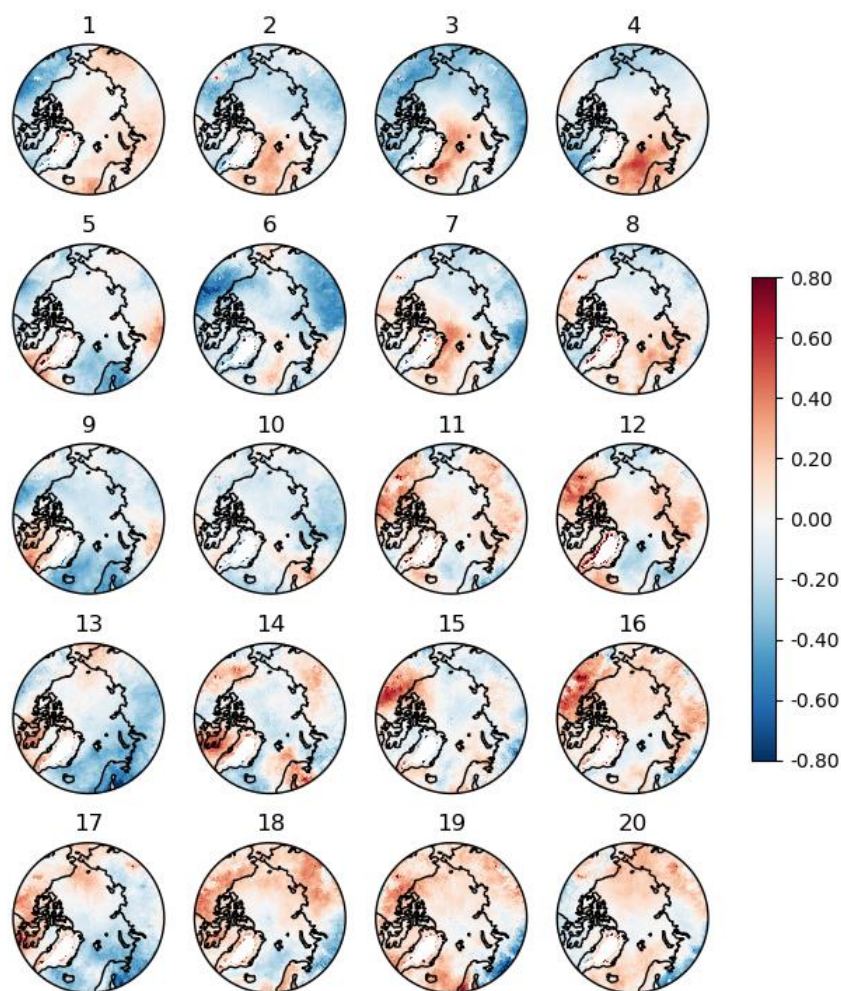
535

536 Fig. 2: Mean sea level pressure (MSLP) averaged over the cases belonging to each of the 20  
537 circulation types.

538

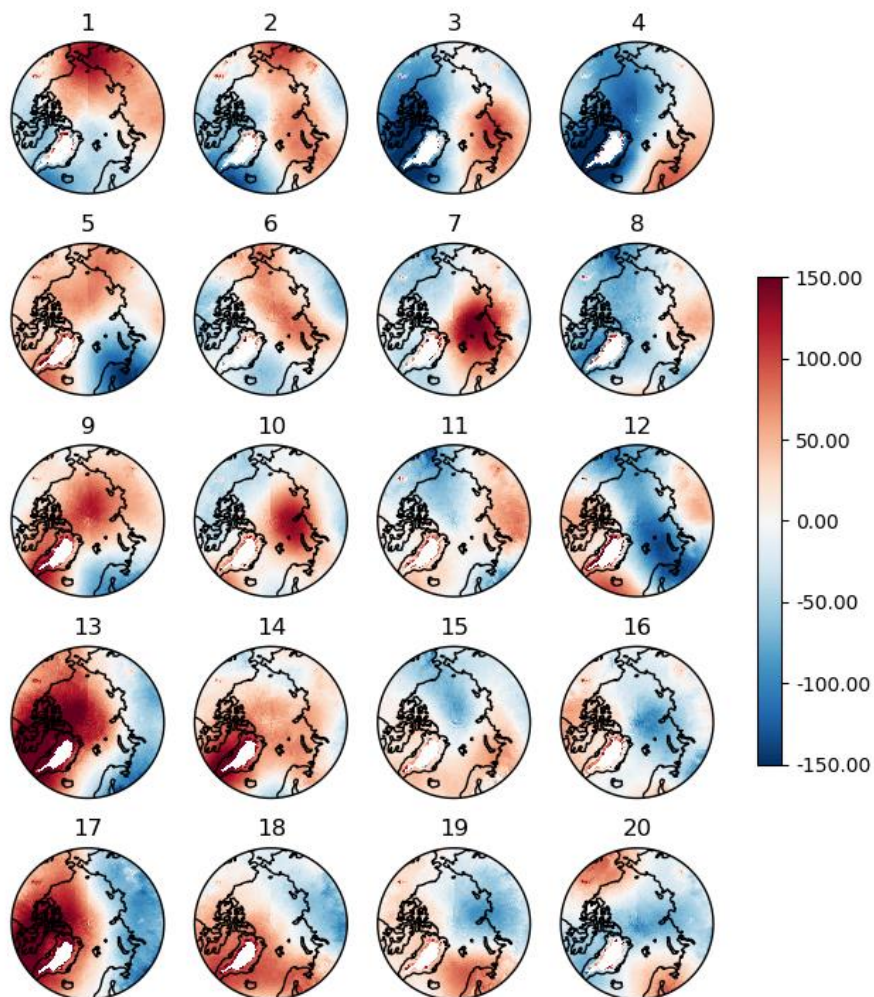


539



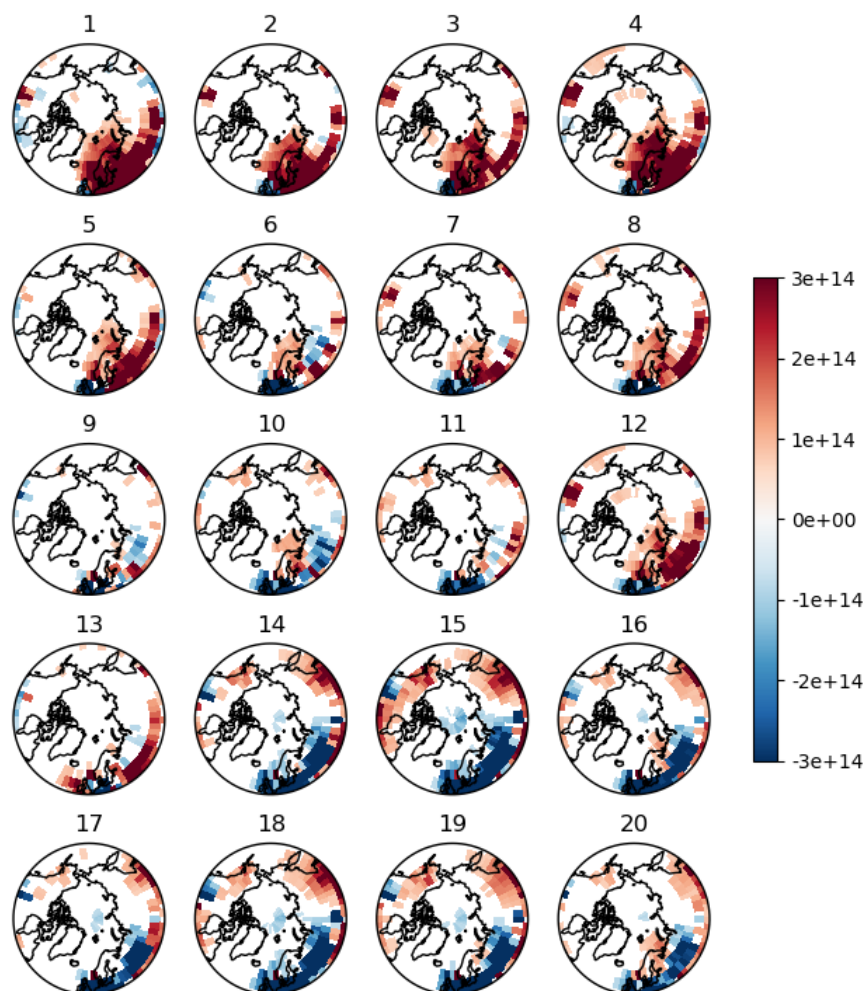
540

541 Fig. 3: The specific humidity anomalies ( $\text{g kg}^{-1}$ ) at 850 hPa based on the AIRS data in the 20 circulation  
542 types.



543

544 Fig. 4: The geopotential height anomalies (in m) at 500 hPa based on the AIRS data in the 20  
545 circulation types



546

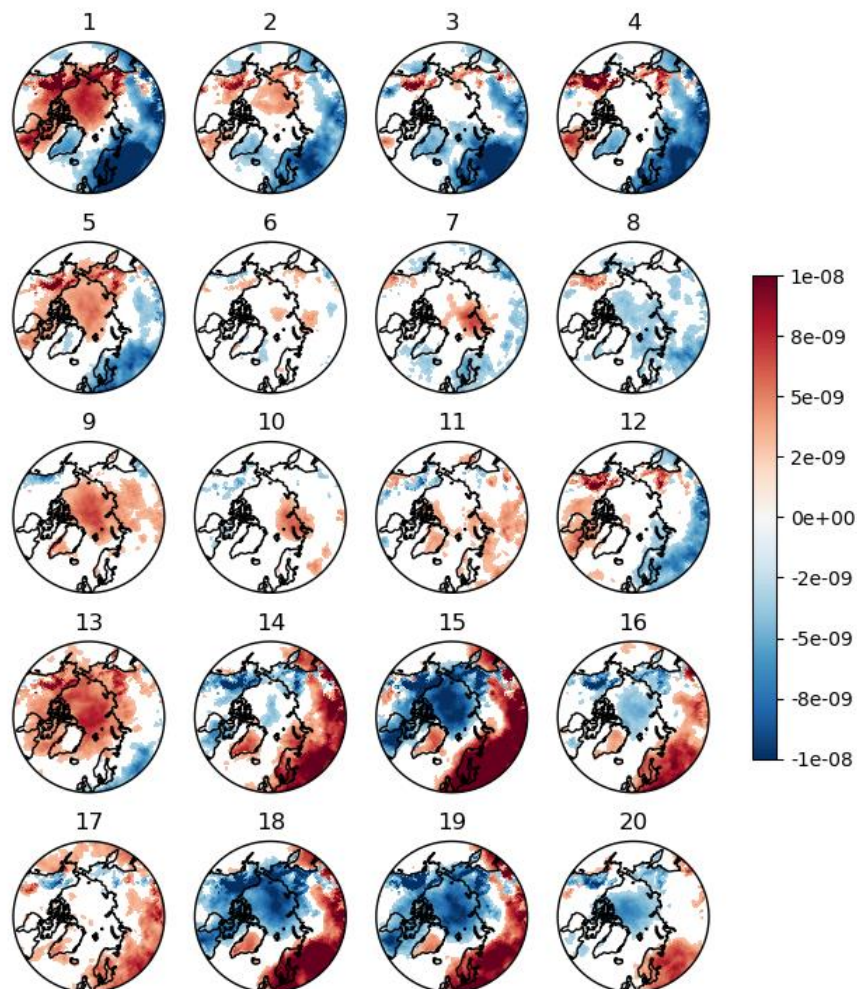
547 Fig. 5: The NO<sub>2</sub> total column anomalies (molec/cm<sup>2</sup>) based on OMI data in the 20 circulation types.

548 Only those anomalies that are statistically significant at 90% confidence are shown.

549



O<sub>3</sub> anomalies, 925 hPa



550

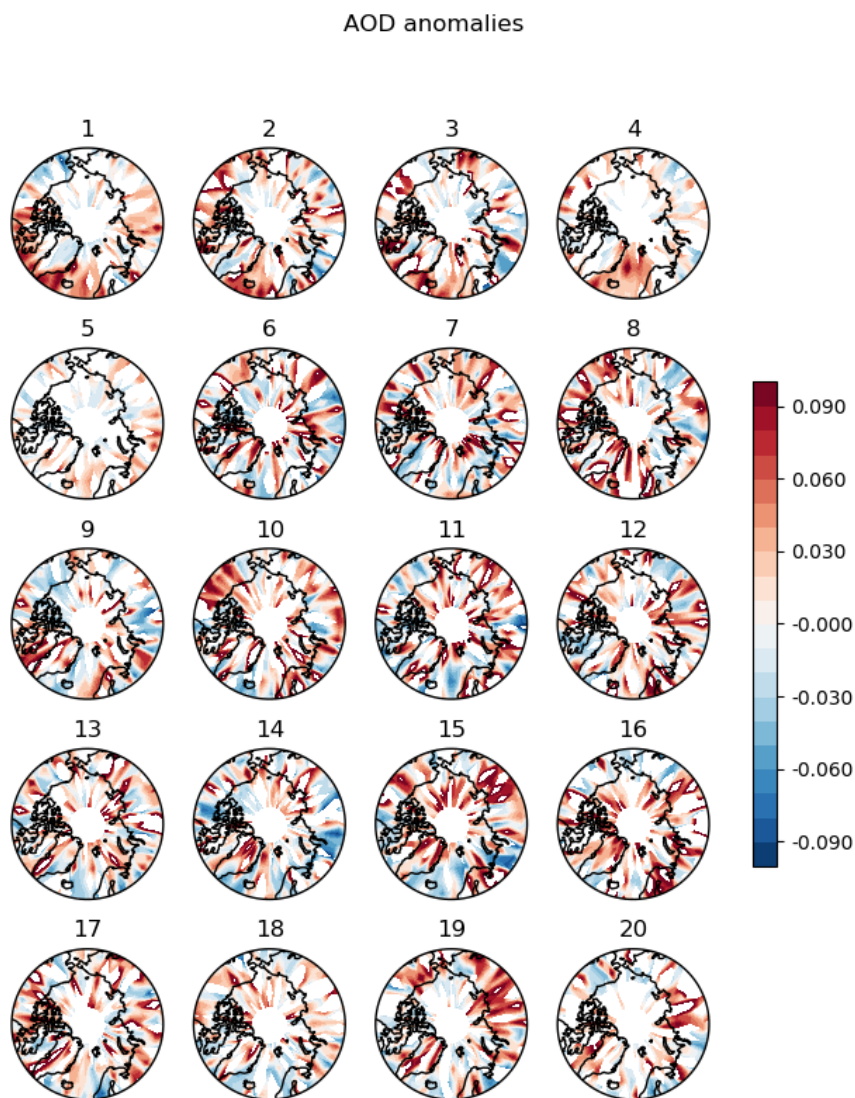
551 Fig. 6: The O<sub>3</sub> anomalies at 925 hPa based on the CAMS data in the 20 circulation types. Only those  
552 anomalies that are statistically significant at 90% confidence are shown.

553

554



555

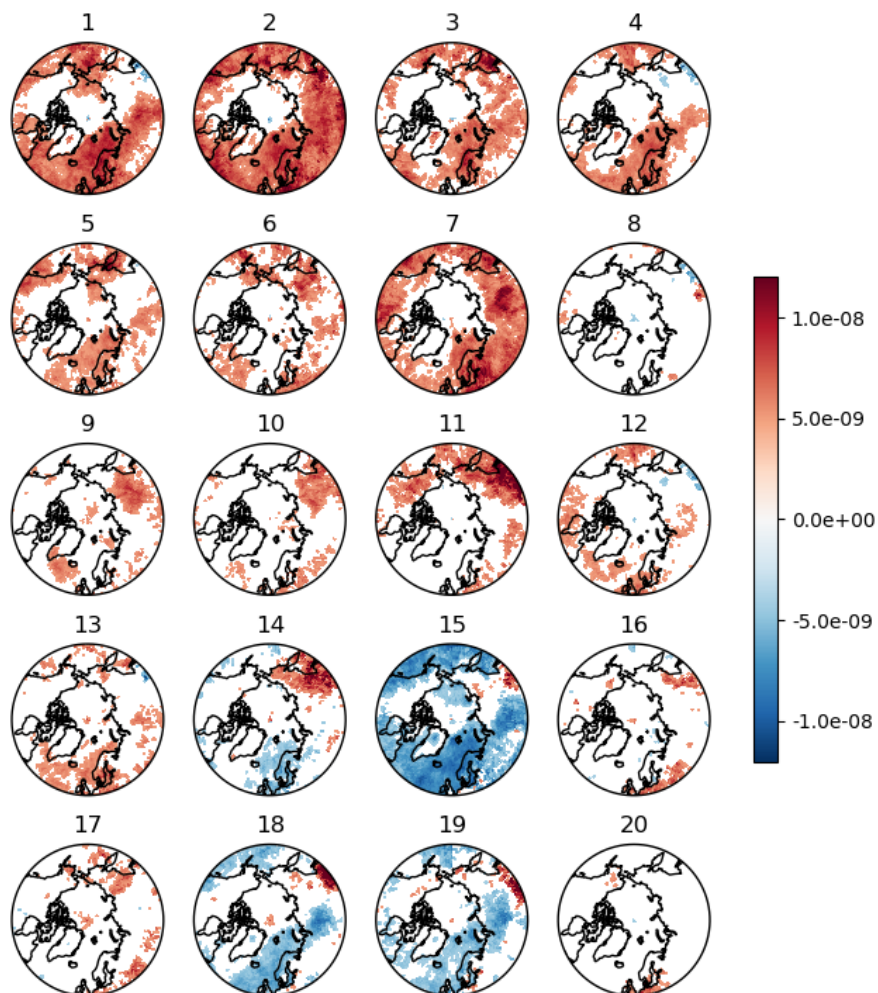


556

557 Fig. 7: The tropospheric AOD anomalies based on the CALIOP-CALIPSO data in the 20 circulation  
558 types with 90% confidence.

559





560

561 Fig. 8: The CO volume mixing ratio anomalies at 500 hPa based on the AIRS data the 20 circulation  
562 types with 90% confidence.

563